



Original article

Investigation on the droplet combustion in rotatory natural convection

J. Dgheim^{*}, A. Chahine, J. Nahed

Laboratory of Applied Physics (LPA), Group of Mechanical, Thermal & Renewable Energies (GMTER), Lebanese University, Faculty of Sciences, Lebanon

ARTICLE INFO

Article history:

Received 17 January 2018

Accepted 19 February 2018

Available online 21 February 2018

Keywords:

Combustion rate

Flame

Evaporation rate

Dgheim number

Droplet combustion

ABSTRACT

Thermal and fluid flow analysis of hydrocarbon liquid droplet evaporation and combustion, in natural convection and in rotation are studied numerically and experimentally. The regression of the liquid droplet square diameter, the evolution of the surface temperature, the temperature variation in liquid and vapor phases, the velocity variation in vapor phase, and the flame radius and temperature evolutions in rotatory natural convection, are determined numerically by using the implicit finite difference scheme and Thomas algorithm. Comparison between numerical and experimental results shows qualitative and quantitative satisfactory agreement. Correlation expressing the combustion rate in function of Dgheim, Prandtl, and Grashof numbers is proposed. The combustion rate is the sum of the initial rate without convection, the combustion rate due to stagnant natural convection and the combustion rate due to rotatory natural convection.

© 2018 Production and hosting by Elsevier B.V. on behalf of King Saud University. This is an open access article under the CC BY-NC-ND license (<http://creativecommons.org/licenses/by-nc-nd/4.0/>).

1. Introduction

The evaporation and combustion of hydrocarbon liquid droplets are used in many industrial systems such as internal combustion of the engine. These phenomena are generally complex, because the interactions between them produce different physical mechanisms. Consequently, it is advantageous to study the combustion of the liquid droplets in configurations as simple as possible so that the physical phenomenon can be observed by eliminating the different influenced parameters. Droplets are usually produced in the form of spray, which often burns in groups rather than individually. However, its technical applicability to spraying is very limited, and the combustion of a single droplet is often studied (Abramzon and Sirignano, 1987).

The evaporation phenomenon of isolated droplets has been studied by many researchers (Abdel-Qader and Hallett, 2005; Vysokomornaya et al., 2017). The regression of the droplet radius and the evolution of the droplet surface temperature are considered by several researchers (Bhattacharya et al., 1996; Bouaziz et al., 2001; Merouane and Bounif, 2010). These authors studied

numerically and experimentally the evaporation of the droplets in natural and forced convection. In their studies, the d^2 law is verified.

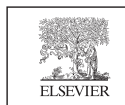
The fluid flow equations were solved (Deplanque and Sirignano, 1993) using finites differences method. The most recent developments in the modeling of heating and evaporation of fuel droplets are reviewed (Sazhin, 2017). The author discussed and analyzed the different models concerning the evaporation of a stagnant droplet. The equations of the heat and mass transfer of a rotating hexane droplet in evaporation were solved numerically (Dgheim et al., 2012). The authors determined the thickness of the boundary layer and the heat and mass transfers' dimensionless parameters.

The combustion rate of monocomponent liquid droplets was studied by Xu et al. (2004). The authors determine the combustion rate as a function of Reynolds number. They studied the influence of the room temperature and the initial droplet radius on the combustion rate. The model dealing with heating and evaporating of fuel droplets, taking into consideration the effects of the finite thermal conductivity was studied (Elwardany et al., 2016; Dgheim et al., 2017). In addition, the evaporation of rotating hydrocarbons droplet in forced convection was studied (Dgheim et al., 2013). The authors proposed the Dgheim number (DG) which is a dimensionless number relevant in the study of fluid transport phenomena in fluid flows. An experimental study on the evaporation rates of a liquid hydrocarbon droplet in natural convection was considered by many authors (Kelly-Zion et al., 2009; Subbarayan et al., 2016). They determined the evaporation rate by using the regression of the stagnant droplet diameter.

^{*} Corresponding author.

E-mail address: jdgheim@ul.edu.lb (J. Dgheim).

Peer review under responsibility of King Saud University.



Production and hosting by Elsevier

Nomenclature

B	Spalding transfer number
C_p	heat capacity at constant pressure, $\text{J.kg}^{-1}.\text{K}^{-1}$
d	droplet diameter, m
DG	Dgheim number
g	gravity acceleration, m.s^{-2}
Gr	Grashof number
q	heat quantity, J.kg^{-1}
K	combustion rate, $\text{m}^2.\text{s}^{-1}$
L	latent heat of evaporation, J.kg^{-1}
Le	Lewis number
\dot{m}	mass flow, $\text{kg.m}^{-3}.\text{s}^{-1}$
Nu	Nusselt number
P	pressure, Pa
Pr	Prandtl number
r	droplet radius, m
Sc	Schmidt number
Sh	Sherwood number
Sig	Molar Mass rate
t	time, s
T	temperature, K
U	velocity, rd.s^{-1}
V	rotation velocity, m/s
Vr	rotation velocity, rd.s^{-1}
ω	rotation velocity, rps
Y	Mass fraction

Greek letters

α	thermal diffusivity, $\text{m}^2.\text{s}^{-1}$
β	expansion coefficient
γ	kinematic viscosity, $\text{m}^2.\text{s}^{-1}$

η	dimensionless radius
λ	thermal conductivity, $\text{W.K}^{-1}.\text{m}^{-1}$
μ	dynamic viscosity, $\text{kg.m}^{-1}.\text{s}^{-1}$
ρ	density, kg.m^{-3}

Subscripts

∞	ambient
a	air
crit	critical
ebn	Boiling
f	fuel
F	flame
fT	heat transfer limit
fM	mass transfer limit
g	gas
j	component index
l	liquid
L	linear
M	mass
O	initial
R	chemical reaction
S	surface
T	Thermal
v	vapor
vs	saturated steam

Superscripts

*	dimensionless values
---	----------------------

However, the fuel ignition in the engines is difficult to control. Thus, making accurate fuel combustion models is a necessity for design improvements. The heptane component is an important fuel being researched for this purpose, due to its similarity to diesel fuel standard composition (Gauthier et al., 2004). The combustion rate of the rotating heptane droplets have not been deeply developed by the researchers, despite their multiple applications and utility in the scientific committee.

2. Mathematical model

Our mathematical model uses the heat and fluid flow transfers equations in the vapor phase and the heat transfer equation in the liquid phase of the hydrocarbon liquid droplet. The isolated droplet of radius r_s is considered as a saturated sphere with heptane component. It is evaporated and burned in an ambient medium under the effect of the rotating natural convection.

Fig. 1 shows the liquid evaporation process. The liquid droplet rotates around its vertical axis in natural convection. The ambient pressure is supposed to be equal to one atmosphere. Our model is based on the film theory (Abramzon and Sirignano, 1987). In this theory, heat and mass transfers between the droplet surface and the external gas happens inside a thin gaseous film surrounding the rotating droplet. Moreover, it assumes laminar and steady flow around the rotating sphere and neglects surface tension, chemical reaction, radiation, and Soret and Dufour effects.

In the vapor phase ($r_{sj} \leq r_j \leq r_{gi}$), the conservation equations are the following:

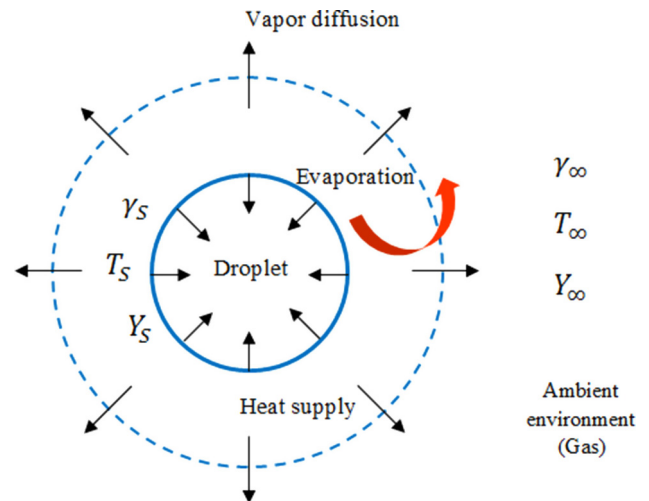


Fig. 1. Liquid droplet evaporation.

The energy conservation equation:

$$\frac{\partial T_g}{\partial t} + U_g \frac{\partial T_g}{\partial r} = \frac{1}{\rho_g C_{p_g} r_j^2} \frac{\partial}{\partial r} \left(\lambda_g r_j^2 \frac{\partial T_g}{\partial r} \right) + \frac{\dot{m}_{lj}}{\rho_g} (T_g - T_s) \quad (1)$$

The fluid flow conservation equation:

$$\frac{\partial U_g}{\partial t} + U_g \frac{\partial U_g}{\partial r} = \frac{1}{\rho_g C_{p_g} r_j^2} \frac{\partial}{\partial r} \left(\mu_g r_j^2 \frac{\partial U_g}{\partial r} \right) - g \beta_T (T_g - T_\infty) \quad (2)$$

The evaporation of the droplet is subject to the action of two phenomena. The first one is the normal evaporation of a droplet placed in an ambient environment, and the second one is the evaporation under the effect of the rotation:

$$\dot{m}_{lj} = \frac{3\rho_l}{r_j} \frac{\partial r_j}{\partial t} + \frac{3\rho_l\omega}{2\pi} \quad (3)$$

In the liquid phase ($r_{0j} \leq r_j \leq r_{sj}$), the energy conservation equation is the following:

$$\frac{\partial T_l}{\partial t} = \frac{1}{\rho_l C_{pl} r_j^2} \frac{\partial}{\partial r} \left(\lambda_l r_j^2 \frac{\partial T_l}{\partial r} \right) \quad (4)$$

The variables (t, r) are transformed to ($t, \eta = r/r_s$), to avoid the non-uniformity of the mesh spacing near the droplet surface, namely:

$$\frac{\partial}{\partial t} \Big|_{t,r} = \frac{\partial}{\partial t} - \frac{\eta}{r_s} \frac{dr_s}{dt} \frac{\partial}{\partial \eta}; \quad \frac{\partial}{\partial r} \Big|_{t,r} = \frac{1}{r_s} \frac{\partial}{\partial \eta}; \quad \frac{\partial^2}{\partial r^2} \Big|_{t,r} = \frac{1}{r_s^2} \frac{\partial^2}{\partial \eta^2} \quad (5)$$

Therefore, the transfers' equations in the vapor phase become:

$$\frac{\partial T_g}{\partial t} = \frac{\alpha_g}{r_{sj}^2} \left(\frac{2}{\eta} - \frac{r_{sj}}{\alpha_g} U_g + \frac{\eta r_{sj}}{\alpha_g} \frac{dr_{sj}}{dt} + \frac{1}{\lambda_g} \frac{\partial \lambda_g}{\partial \eta} \right) \frac{\partial T_g}{\partial \eta} + \frac{\alpha_g}{r_{sj}^2} \frac{\partial^2 T_g}{\partial \eta^2} + \frac{\dot{m}_{lj}}{\rho_g} \times (T_g - T_s) \quad (6)$$

$$\frac{\partial U_g}{\partial t} = \frac{\gamma_g}{r_{sj}^2} \left(\frac{2}{\eta} - \frac{r_{sj}}{\gamma_g} U_g + \frac{\eta r_{sj}}{\gamma_g} \frac{dr_{sj}}{dt} + \frac{1}{\mu_g} \frac{\partial \mu_g}{\partial \eta} \right) \frac{\partial U_g}{\partial \eta} + \frac{\gamma_g}{r_{sj}^2} \frac{\partial^2 U_g}{\partial \eta^2} - g\beta_r(T_g - T_\infty) \quad (7)$$

The total mass flow becomes:

$$\dot{m}_{lj} = 3 \frac{\rho_l}{\eta} \left(\frac{\partial \eta}{\partial t} - \frac{\eta}{r_{sj}} \frac{dr_{sj}}{dt} \right) + \frac{3\rho_l\omega}{2\pi} \quad (8)$$

The heat transfer equation in the liquid phase becomes:

$$\frac{\partial T_l}{\partial t} = \frac{\alpha_l}{r_{sj}^2} \left(\frac{2}{\eta} + \frac{\eta r_{sj}}{\alpha_l} \frac{dr_{sj}}{dt} + \frac{1}{\lambda_l} \frac{\partial \lambda_l}{\partial \eta} \right) \frac{\partial T_l}{\partial \eta} + \frac{\alpha_l}{r_{sj}^2} \frac{\partial^2 T_l}{\partial \eta^2} \quad (9)$$

To complete our mathematical model, the following initial, and boundary conditions are used: Initial conditions: $\forall t < t_0$

Inside the liquid phase: $T_l = T_{L0}$

At the surface of the liquid droplet, the temperature and mass fraction are equals respectively to the rotating droplet surface temperature and surface mass fraction. The surface mass fraction varies according to the saturated vapor pressure determined by Clausius Clapeyron equation (Abramzon and Sirignano, 1987). Therefore: $T_s = T_{S0}$

$$Y_{Sj} = Y_{S0j} = \frac{P_{VS}}{\left(P_{VS} + \frac{(P_\infty - P_{VS})M_a}{M_f} \right)} \quad (10)$$

In the vapor phase: $T_g = T_\infty, U_g = 0$

The latent heat of vaporization is written as the following (Dgheim et al., 2013):

$$L = L_v \left(\frac{(T_{crit} - T_s)}{(T_{crit} - T_{ebn})} \right)^{0.38} \quad (11)$$

Boundary conditions: $\forall t > t_0$

At the droplet center ($\eta = 0$):

$$\frac{\partial T_{lj}}{\partial \eta} \Big|_{ce} = 0 \quad (12)$$

At the droplet surface ($\eta = 1$):

The continuity of conduction, convection and evaporation is applied:

$$\lambda_g \left(\frac{\partial T_g}{\eta \partial \eta} \right)_s = \lambda_l \left(\frac{\partial T_l}{\eta \partial \eta} \right)_s + \dot{m}_{lj} q_g r_s^2 \quad (13)$$

And the vapor velocity is taken equal to: $U_g = 0$

In our model, correlations of Nusselt and Sherwood numbers for the combustion of a liquid droplet in natural convection are used (Dgheim et al., 2001):

$$Nu = 1.31 Gr_T^{0.26} Pr^{0.33} \quad (14)$$

$$Sh_j = 0.93 Gr_{Mj}^{0.25} Sc^{0.15} \quad (15)$$

Mass and thermal balances are always verified at the droplet's surface. The external radii that are defined by Abramzon and Sirignano, depend on the modified Nusselt and Sherwood numbers:

$$r_{Tr} = \frac{r_s Nu^*}{Nu^* - 2} \quad (16)$$

$$r_{Mj} = \frac{r_s Sh_j^*}{Sh_j^* - 2} \quad (17)$$

This model uses the relationships proposed by Abramzon and Sirignano, as the following:

$$Nu^* = Nu \frac{\ln(1 + B_T)}{B_T} \quad (18)$$

$$Sh_j^* = Sh_j \frac{\ln(1 + B_M)}{B_M} \quad (19)$$

The viscosity, the density, the thermal conductivity, the specific heat, the coefficient of diffusion of the air-fuel mixture and the latent heat of vaporization are computed using the literature (Lieberam, 1993; Abramzon and Sirignano, 1987; Dgheim et al., 2017). These correlations show that the thermo-physical and transport properties are dependent at each node on the average temperature as the following:

$$\bar{T} = T_s + \frac{T_F - T_s}{3} \quad (20)$$

The heat balance of the flame (Fig. 2) is written as the following equation:

Heat of combustion

+ Heat transfer red to the surrounding environment

= Heat transferred to the droplet

+ Heat of the droplet evaporation

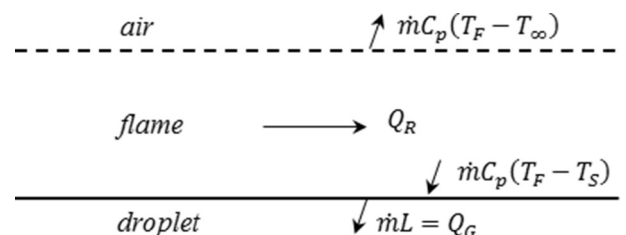


Fig. 2. Diagram of the flame heat balance.

Thus, the temperature of the flame is written as:

$$T_F = \left\{ T_S + \frac{q_R - q_g}{Cp_g} + \frac{Cp_g T_\infty}{Cp_g \left[\left(1 - \frac{Y_\infty}{Sig} \right)^{1/Le} - 1 \right]} \right\} \times \left\{ 1 + \frac{Cp_g}{Cp_g \left[\left(1 - \frac{Y_\infty}{Sig} \right)^{1/Le} - 1 \right]} \right\}^{-1} \quad (21)$$

The boundary layer ignition criterion is used for the gas mixture ignition. It assumes the ignition of hot gaseous mixture when the local temperature exceeds the minimum ignition temperature of the heptane.

The flame radius is given by the following formula (Abramzon and Sirignano, 1987):

$$R_{Fj} = r_{Sj} Sh_j \log(1 + B_M) \left[2 \log \left(\frac{Y_\infty + Sig}{Sig} \right) \right]^{-1} \quad (22)$$

The transfers' equations in the liquid and vapor phases are schemed using an implicit finite difference method. A preliminary study of the calculus stability for a given space step $\Delta\eta$ in both phases liquid and vapor, leads to a time step $\Delta t = 0.1$ s. The value of these steps leads to a scheme of 181×7001 . The system of the algebraic equation has been solved by using Thomas algorithm.

3. Experimental setup

The experimental process allows us to study the evaporation and the combustion, at atmospheric pressure, of a liquid fuel droplet in natural convection.

3.1. The experimental device

The study of the evaporation or combustion of a droplet at atmospheric pressure is carried out in a rectangular test section ($15 \times 20 \times 20$ cm³) that ensures the natural convection. In the test section, the average rotating velocity that is varying between 0 and 8 rps, is generated by an electrical motor linked to a frequency generator (Fig. 3). The droplets are suspended at the free end of the tube of quartz (0.1 mm), using a micrometric syringe with a needle of 0.4 mm diameter. The quartz tube is linked to an electrical motor and a frequency generator to rotate the hydrocarbon liquid droplet. The combustion phenomena are realized by a spark ignition. The thermocouple of type K of 1 mm of diameter is used to measure the test section temperature. The infrared thermometer

of spectral response 8–14 μ m is used to measure the initial surface temperature of the liquid droplet by adding the heptane emissivity which is equal to 0.95. The LED lamp allows illuminating the vein of experimentation.

3.2. Calibration of video camera

The conversion ratio of the pixel to the dimensional unit is determined by the following procedure: First, images of a capillary of known diameter ($d \approx 1.8$ mm) are recorded by the Hero Pro camera in two horizontal and vertical positions. Then, image processing provides the horizontal ratio R_x ($R_x = N_{\text{pixel_droplet}} \times \text{horizontal length}/320$ pixel) and vertical ratio R_y ($R_y = N_{\text{pixel_droplet}} \times \text{vertical length}/240$ pixel). The same procedure is performed for each position change of the camera.

3.3. System and image processing

The durations of droplet evaporation or burning are recorded by a video system camera. The video system consists of a camera video with a suitable optics, a recorder and a PC to visualize the phenomenon. The camera allows us to view 60 images/s. The spatial definition of an image after decompression is 320×240 pixels. The droplet in evaporation or combustion requires a high luminous contrast that is obtained by illuminating the back of the experimental vein. Thus, on the screen of the computer, the droplet appears opaque on a white background. This experimental procedure facilitates the extractions of the droplet contour, which is obtained by scanning and detecting the black pixel of each image line by line. Later, the maximum black pixel line that's equivalent to the droplet diameter is given. The equivalent diameter of the droplet is determined to initialize the numerical model and to obtain the diameter regression versus time.

3.4. Rotating system of the liquid droplet

An optical tachometer and a reflected tape placed on the needle that carries the droplet are used to measure the rotating velocity in revolution per minute (rpm). Thus, by increasing the voltage value of the frequency generator, the rotating velocity increases. These results are expressed by the following equations and given in the Table 1:

$$Vr_{(rd/s)} = \frac{V_{(m/s)}}{r_{(m)}} \quad (23)$$

where $\omega_{(rpm)} = Vr_{(rd/s)} \times 60/2\pi$.

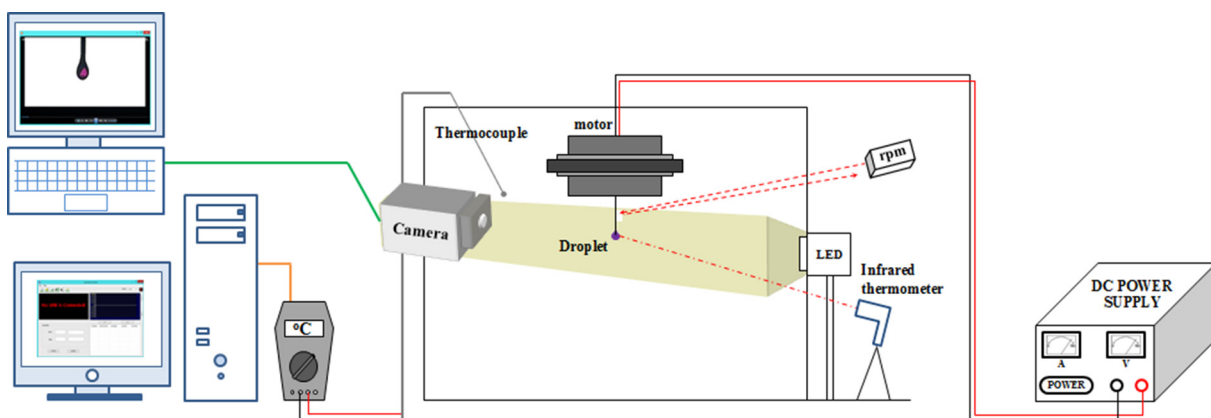


Fig. 3. Experimental setup.

Table 1
Measurement of the rotating velocity of the electrical motor.

Current I (A)	Voltage U (V)	Measured Speed ω (rpm)	Vr (rd/s)
0.03	1.00	180	18.85
0.03	1.20	300	31.42
0.03	1.40	420	44.00

4. Results and discussion

The computations are performed for a rotating heptane droplet of initial radius varying between 0.35 mm and 0.75 mm. The ambient pressure is one atmosphere, whereas the ambient temperature varies between 300 K and 500 K. The rotational velocity varies between 0 and 50 rps.

4.1. Model accuracy

In evaporation, in stagnant natural convection, the regression of the square radius of the heptane droplet is presented numerically and experimentally. The square of the droplet radius decreases gradually until the liquid droplet evaporates completely. The results of our numerical model for a heptane droplet (Fig. 4) are compared, under the same conditions, with the experimental results obtained by our experimental setup and satisfactory qualitative and quantitative agreements are observed. The relative error is less than 10%. Moreover, these results show that the large droplet takes longer time to evaporate completely.

Then, the evaporation, in rotatory natural convection, of the heptane droplet is studied numerically and experimentally. The comparison between the numerical and experimental results at several rotating velocities also shows satisfactory qualitative and quantitative agreements. The influence of the rotation velocity on the regression of the droplet square radius, evaporating in natural convection is clearly shown in Fig. 5. When the velocity of rotation of the liquid droplet is increased, the evaporation rate increases, which accelerates the evaporation process of the latter (the evaporation time decreases). Another comparison between stagnant and rotating droplets is presented in the same figure in order to better observe the influence of the rotatory natural convection. The obtained results for the rotating droplets show clearly higher

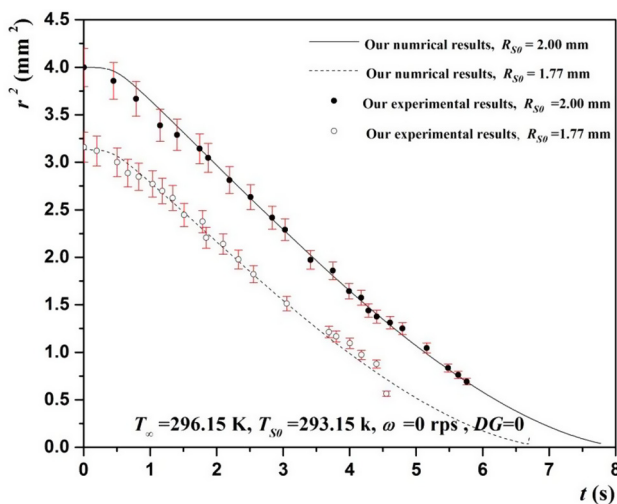


Fig. 4. Comparison between our numerical and experimental results for the regression of the square radius of the heptane droplet in evaporation in stagnant natural convection.

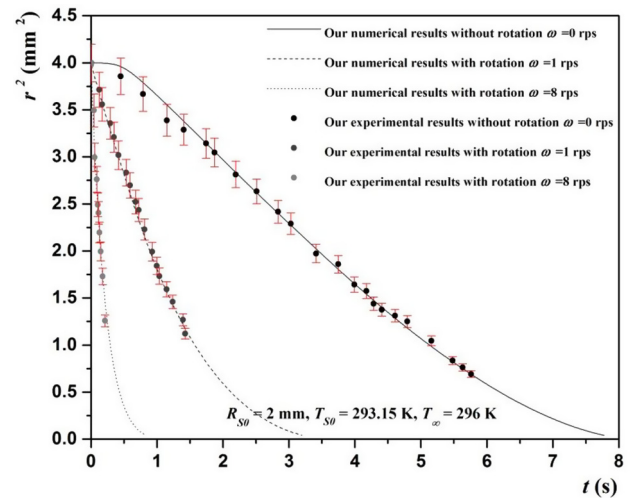


Fig. 5. Comparison between our numerical and experimental results for the regression of the square radius of the heptane droplet in evaporation in rotatory natural convection.

evaporation rate than the one of the stagnant droplet. The video frames of investigated process are presented in Fig. 6.

Moreover, the combustion of a stagnant heptane droplet, in natural convection, is studied numerically and experimentally (Fig. 7). The liquid droplet evaporates under the effect of the high temperature of the gaseous phase, and decreases progressively with the evolution of the combustion time by verifying the d^2 law. A concordance between the results of the numerical model and those obtained experimentally is clearly observed. The small difference comes from the systematic and random error (error less than 10%).

4.2. Physical parameters development for rotating hydrocarbon droplet combustion

After the validation of our numerical model, the influence of the physical parameters (initial droplet radius, velocity of rotation, and ambient temperature) on the combustion of a heptane droplet in rotatory natural convection is studied numerically.

The influence of the rotating velocity on the droplet surface temperature evolution of the burning of a heptane droplet in rotatory natural convection (Fig. 8). This figure shows that the increase of the droplet rotating velocity accelerates the combustion phenomenon by reducing the time of combustion process. Thus, the droplet surface temperature increases by remaining inferior than the boiling temperature of the heptane component. However, the increase of the rotating velocity does not greatly influence the time evolution of the surface temperature of the heptane droplet since the latter rapidly reaches its temperature of saturation. The fast increase of the surface temperature of the liquid droplet results from the effect of the high temperature of the gaseous phase (flame temperature) that generates a large thermal gradient between the gaseous and the liquid phases, accelerating the evaporation of the latter. Moreover, the Dgheim dimensionless number increases with the increasing of the rotating velocity and the combustion rate ($DG = 0.508$ for $Vr = 50$ rd/s) by improving the combustion processes.

The influence of the rotating velocity on the flame radius and temperature of a heptane droplet in rotatory natural convection is presented in Figs. 9 and 10 respectively. It is noted that, at the beginning of the combustion process, the dimensionless radius of the flame (Fig. 9) increases rapidly over time to reach a maximum value near the liquid droplet. Then, it gradually decreases to reach



Fig. 6. Heptane droplet evaporation process.

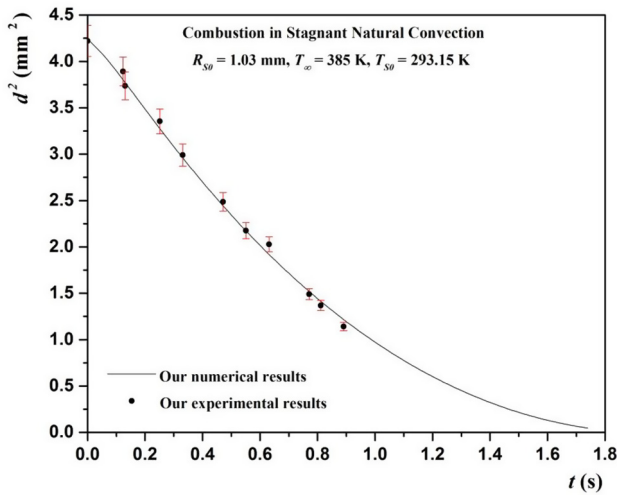


Fig. 7. Comparison between our numerical and experimental results for the regression of the square diameter of the heptane droplet in combustion in stagnant natural convection.

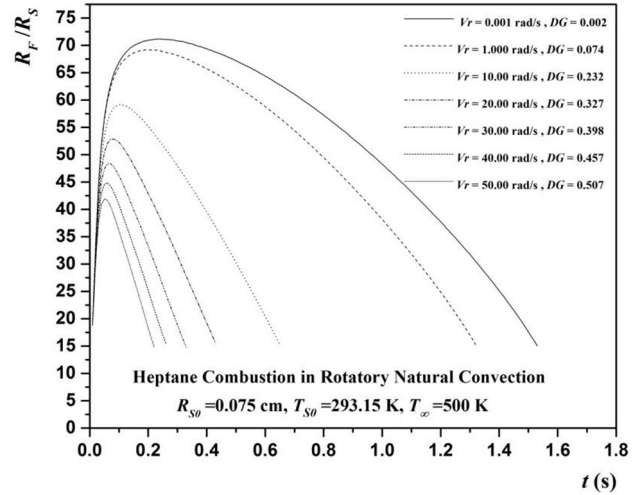


Fig. 9. Time evolution of the flame radius rate of the heptane droplet, in combustion, in rotary natural convection, for different rotating velocities.

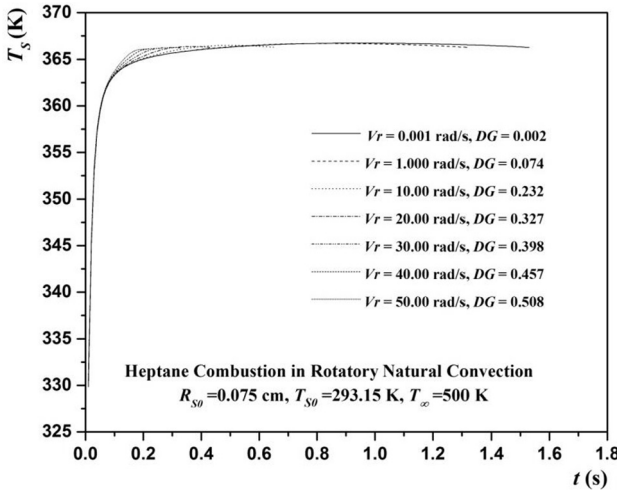


Fig. 8. Time evolution of the heptane droplet surface temperature, in combustion, in rotary natural convection, for different rotating velocities.

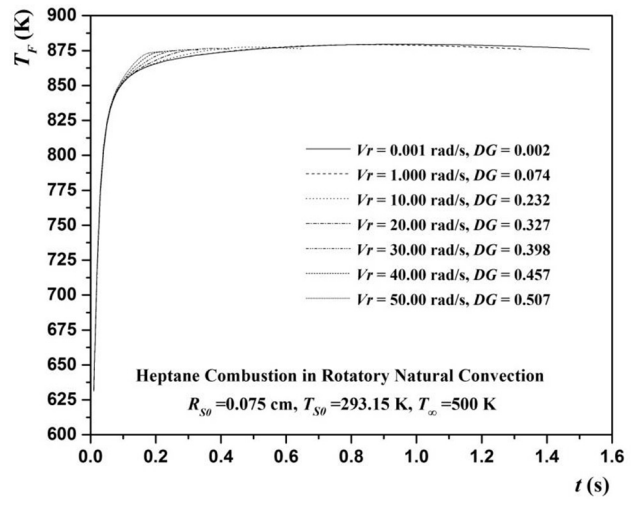


Fig. 10. Time evolution of the flame temperature of the heptane droplet, in combustion, in rotary natural convection, for different rotating velocities.

a minimum value of 0.11 cm distant from the liquid droplet. This increase is logical in view of the fact that the ignition of the vapor in the vicinity of the hydrocarbon droplet gives rise to a flame, which develops rapidly to reach its maximum limit, and it is gradually extinguished with the total evaporation of the heptane droplet. By increasing the rotating velocity of the heptane droplet,

the combustion phenomenon accelerates, and the radius of the flame, which reaches approximately 70 times the dimension of the droplet radius, decreases. At the same time, the temperature of the flame, starting from the boiling temperature, undergoes a rapid increase to reach its maximum value, and then it goes down to reach the surface temperature of the flame (Fig. 10). The

influence of the rotating velocity on the temperature of the flame is minimal, since the latter cannot greatly exceed the ignition temperature of the heptane droplet.

The evolution of the radial velocity in the heptane’s vapor phase, in combustion, in rotatory natural convection is presented (Fig. 11). The radial velocity of the vapor phase increases from its initial value at the liquid – vapor interface to reach its maximum value. This increase is due to the heat and mass transfer caused by the burning of the heptane droplet gaseous phase. This phenomenon is caused by the high thermal and mass gradients between the liquid and gaseous phases on the one hand and between the inflamed gas phase and the ambient medium on the other hand. The radial velocity decreases progressively over time by showing the evolution of the heptane flame radius.

The evolution of the heptane temperature, in combustion, in rotatory natural convection is presented (Fig. 12) for different times. The temperature of the liquid phase of the heptane droplet increases abruptly to reach its interface value determined from the continuity of conduction, convection and evaporation at the surface of the liquid droplet. Then, it continues its evolution in the gaseous phase to reach its maximum value. This increase is due to the thermal and mass transfers generated by the ignition of the gaseous phase of the heptane droplet. These cause a high thermal gradient between the liquid phase and the gas phase on the one hand and between the ignited gas phase and the ambient medium on the other hand. Along time, the temperature profiles follow the flame radius evolution.

The influence of the rotating velocity variation on the temperature of the heptane droplet combustion, in the liquid and gas phases, in rotatory natural convection are studied (Fig. 13). This figure shows part of the results obtained at time $t = 0.25$ s, so that to present the evolution of the temperature around the liquid-vapor interface. In the liquid phase, the temperature increases to reach its interface value corresponding to the surface temperature of the liquid droplet. The surface temperature is determined from the thermal balance applied at the surface of the liquid droplet. Thereafter, the temperature continues to rise to a maximum value corresponding to the maximum value of the heptane flame temperature and then falls down to the surface temperature of the flame. The latter is calculated from the thermal balance applied between the inflamed gas phase and the ambient environment. The initial interface is represented by the initial radius of the liquid droplet, 0.075 cm. By increasing the rotating velocity of the liquid

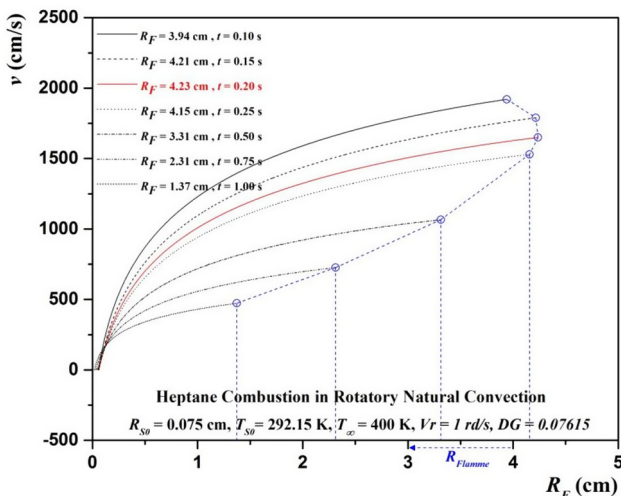


Fig. 11. Radial evolution of the radial velocity of the heptane droplet, in combustion, in rotatory natural convection.

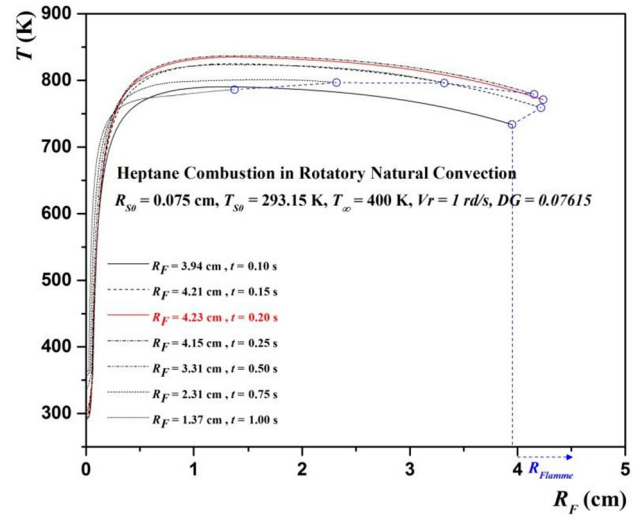


Fig. 12. Radial evolution of the heptane droplet temperature, in combustion, in rotatory natural convection for different times.

droplet, the initial interface begins to decrease by showing the evaporation of the liquid phase and the increase of the temperatures of the liquid and vapor phases. Thus, the increase of the rotating velocity of the liquid droplet increases the temperature gradient between the liquid phase and its interface on the one hand, and between the vapor phase and the ambient medium on the other hand. This gradient rapidly evaporates the heptane liquid droplet. Moreover, Dgheim dimensionless number increases with the increasing of the rotating velocity by showing an augmentation of the transfers between the droplet and its neighborhood.

In order to develop a new correlation for the combustion rate, the influence of the ambient temperature variation on the regression of the square diameter of the heptane droplet, in stagnant natural convection is presented (Fig. 14). Thus, the increasing of the ambient temperature accelerates the combustion process and increases Prandtl (Pr), and thermal Grashof (Gr_T) numbers. Consequently, the burning rate of the heptane droplet, which is the slope corresponding to the regression of the square diameter of the liquid droplet versus time, reaches high values ($K = 1.679$ for $T = 500$ K).

The evolution of the burning rate as a function of Prandtl and thermal Grashof numbers is shown in Fig. 15. The burning rate increases rapidly with increasing thermal Rayleigh number. It reaches stable values for high values of thermal Rayleigh number. The least squares method is used to smooth our numerical results. This method allows us to determine a new correlation expressing the average burning rate as a function of Prandtl and thermal Grashof numbers and the rate without convection. This correlation is expressed by the following equation:

$$K = 0.02725 + 1.00368(Pr \times Gr)^{0.25} \quad (24)$$

where:

$$\frac{K - K_0}{K_0} = 36.83231(Pr \times Gr)^{0.25} \quad (25)$$

where $K_0 = 0.02725$, is being the constant rate for the case without convection.

This correlation takes into consideration the variability of the thermo-physical and transport properties of hydrocarbon liquid droplet, in combustion, in stagnant natural convection.

Then, by rotating the liquid droplet, the combustion rate increases progressively with the increase in the rotation velocity

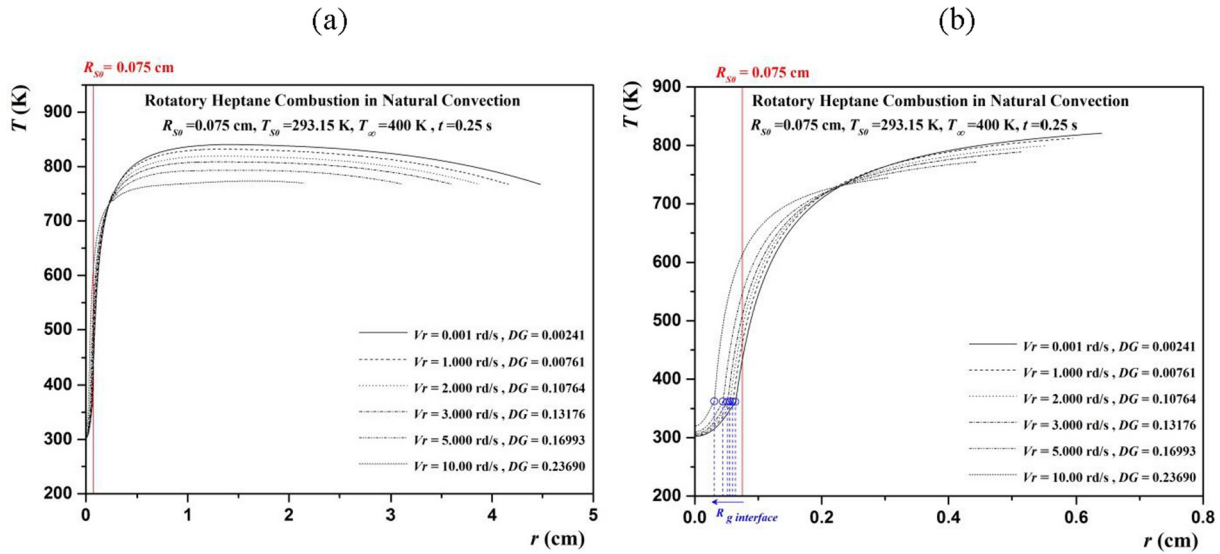


Fig. 13. (a) Radial evolution of the temperature of the heptane droplet, in combustion, in rotatory natural convection, for different rotating velocities. (b) Figure on the left is the zoom of the figure on the right around the liquid-vapor interface.

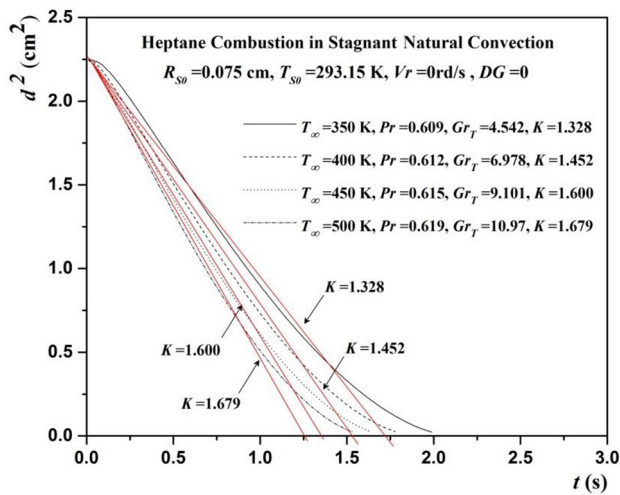


Fig. 14. Time evolution of the regression of the square diameter of the heptane droplet, in combustion, in stagnant natural convection, for different ambient temperatures.

of the latter. A new correlation expressing the average burning rate as a function of Dgheim number is determined using the least squares method (Fig. 16). The resulting mathematical equation of the smoothing is as follows:

$$K = 0.02725 + 1.00368(Pr \times Gr)^{0.25} + 41.6125728(Pr \times Gr)^{0.25}(DG)^2 \quad (26)$$

It is also presented by the following form:

$$\frac{K - K_0}{1.00368(Pr \times Gr)^{0.25}} = 1 + 41.46(DG)^2 \quad (27)$$

This correlation takes into consideration the combustion, in natural convection, of the liquid hydrocarbon droplet, in rotation, where the thermo-physical and transport properties such as thermal conductivity, density, specific heat, dynamic viscosity and diffusion coefficient, are variables. In addition, it takes into consideration the variation in the size of the liquid droplets (initial droplet diameter varies from 0.35 mm to 0.75 mm). For each

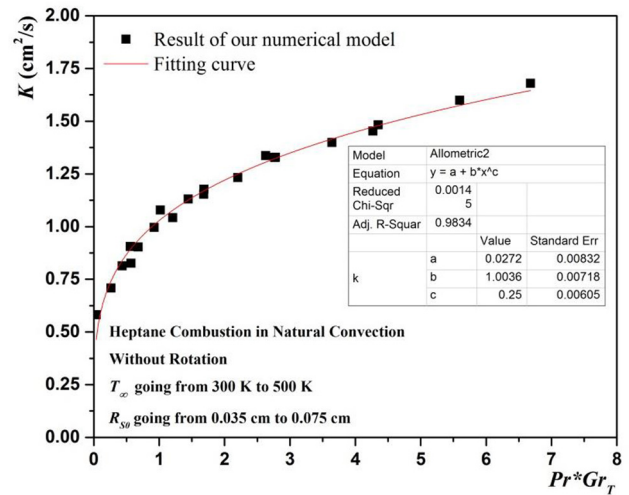


Fig. 15. Burning rate evolution versus Prandtl and thermal Grashof numbers.

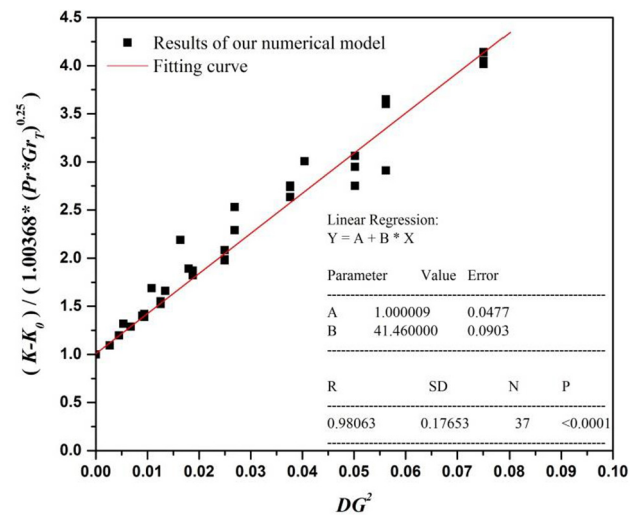


Fig. 16. Burning rate evolution versus square Dgheim number.

droplet diameter, the rotation velocity varies from 1 rd/s to 50 rd/s. Thus, one can deduce that the average combustion rate is the sum of the initial rate without convection, the combustion rate due to stagnant natural convection and the combustion rate due to rotatory natural convection. It also shows that the rotatory convection is preponderant to the stagnant one, so that the effect of the Dgheim number on the combustion of the liquid hydrocarbon droplet in rotation is more important than the effect of the thermal Rayleigh number in stagnant natural convection. The average burning rate reaches values greater than $2 \text{ mm}^2/\text{s}$, whereas it only reaches $1.75 \text{ mm}^2/\text{s}$ for large values of thermal Grashof number for different ambient temperatures. The relative errors between the smoothing curve and the numerical results are less than 10%, which is acceptable numerically.

5. Conclusion

A numerical model describing the heat and fluid flows, that develop in the liquid and vapor phases of the heptane droplet, in combustion, in natural convection, is determined. Our mathematical model introduces the velocity of rotation in the evaporated mass flow to treat the evaporation and combustion of the heptane droplet in rotating natural convection. The experimental study is realized to validate our numerical results and qualitative and quantitative agreements are observed. The obtained results are as follows:

- For small values of Dgheim number, the regression of the heptane droplet square diameter does not strongly follow the d^2 law. But, when Dgheim number increases, the d^2 law is verified and the droplet evaporates rapidly, as the rate of combustion increases with the increase of Dgheim number. In addition, the increase in Dgheim number improves the evaporation process by increasing the droplet surface temperature to reach the boiling temperature of the heptane droplet.
- Temperature and velocity profiles in liquid and vapor phases clearly show the combustion process, the link between both phases, and the evolution of the physical parameters such as the droplet radius regression and the flame radius evolution.
- A new correlation expressing the combustion rate in terms of Dgheim, Prandtl and Grashof numbers and the initial rate (without convection) is proposed.
- The combustion rate is the sum of the initial rate without convection, the combustion rate due to stagnant natural convection and the combustion rate due to rotatory natural convection.
- The effect of Dgheim number on the combustion of the liquid hydrocarbon droplet in rotation is more important than the effect of thermal Rayleigh number in stagnant natural convection.

Acknowledgment

This project is supported by the Lebanese National Council for Scientific Research CNRSL.

References

Abdel-Qader, Z., Hallett, W.L.H., 2005. The role of liquid mixing in evaporation of complex multi-component mixtures: modelling using continuous thermodynamics. *J. Chem. Eng. Sci.* 60, 1629–1640.

- Abramzon, B., Sirignano, W.A., 1987. Approximate theory of a single droplet vaporization in a convective field effect of variable properties. *Stephan flow and transient liquid heating*. Proceedings, ASMEJSME, Thermal Engineering Joint Conference Honolulu.
- Bhattacharya, P., Ghosal, S., Som, S.K., 1996. Evaporation of multi-component liquid fuel droplets. *Int. J. Energy Res.* 20, 385–398.
- Bouaziz, M., Dgheim, J., Bresson, J., Zeghamati, B., 2001. Experimental and numerical study of temperature evolution in evaporation of hydrocarbon droplet. *J. Energy Heat Mass Transfer.* 23, 251–263.
- Deplanque, J.P., Sirignano, W.A., 1993. Numerical study of the transient vaporization of an oxygen droplet at sub and super critical conditions. *Int. J. Heat Mass Transfer.* 36, 4419–4431.
- Dgheim, J., Abdallah, M., Habchi, R., Zakhia, N., 2012. Heat and mass transfer investigation of rotating hydrocarbons droplet which behaves as a hard sphere. *J. Appl. Math. Model.* 36, 2935–2946.
- Dgheim, J., Abdallah, M., Nasr, N., 2013. Evaporation phenomenon past a rotating hydrocarbon droplet of ternary components. *Int. J. Heat Fluid Flow.* 42, 224–235.
- Dgheim, J., Abdallah, M., Nasr, N., 2017. Enhanced evaporation of droplet of ternary component under the effect of thermo-physical and transport properties variability. *Arab. J. Sci. Eng.* 42, 1–14.
- Dgheim, J., Chesneau, X., Pietri, L., Zeghamati, B., 2001. Heat and mass transfer correlation for liquid droplet of a pure fuel in combustion. *J. Heat Mass Transfer.* 38, 543–550.
- Elwardany, A., Sazhin, S.S., Im, H.G., 2016. A new formulation of physical surrogates of FACE A gasoline fuel based on heating and evaporation characteristics. *J. Fuel.* 176, 56–62.
- Gauthier, B.M., Davidson, D.F., Hanson, R.K., 2004. Shock tube determination of ignition delay times in full-blend and surrogate fuel mixtures. *J. Combust. Flame* 139, 300–311.
- Kelly-Zion, P., Pursell, C., Booth, R., VanTilburg, A., 2009. Evaporation rates of pure hydrocarbon liquids under influences of natural convection and diffusion. *Int. J. Heat Mass Transfer.* 52, 3305–3313.
- Lieberam A., VDI, Verlag GmbH, Dusseldorf, Leverkusen. Dc 1–38.
- Merouane, M., Bounif, A., 2010. Theoretical and numerical analysis of fuel droplet vaporization at high temperatures. *Wseas Trans. Heat Mass Transfer* 5, 189–196.
- Sazhin, S., 2017. Modelling of fuel droplet heating and evaporation: recent results and unsolved problems. *Fuel* 196, 69–101.
- Subbarayan, M., Kumaar, J., Padmanaban, M., VanTilburg, A., 2016. Experimental investigation of evaporation rate and exhaust emissions of diesel engine fueled with cotton seed methyl ester and its blend with petro-diesel. *J. Transport Environ.* 48, 369–377.
- Vysokomornaya, O.V., Kuznetsov, G.V., Strizhak, P.A., 2017. Predictive determination of the integral characteristics of evaporation of water droplets in gas media with a varying temperature. *J. Eng. Phys. Thermophys.* 90, 615–624.
- Xu, G., Ikegami, M., Honma, S., Ikeda, K., Dietrich, D.L., Struk, P.M., 2004. Interactive influences of convective flow and initial droplet diameter on isolated droplet burning rate. *Int. J. Heat Mass Transfer.* 47, 2029–2035.

Joseph Dgheim received his teaching diploma in Physics from the Lebanese University in 1997 and his Master degree in Materials and Energetic from Perpignan University in 1998. He received his PhD degree in Hydrocarbons Droplet Combustion from Perpignan University in 2001. He was a postdoctoral research associate at Perpignan University in 2002. He joined the Lebanese University as an associated Professor at the Department of Physics and was promoted to Professor in 2008. His research activities primarily involve the evaporation and the combustion of the rotating hydrocarbons droplets, the nanomaterials and the laser materials interaction. In his career, he received several scholarships and fellowships.

Jean Nahed completed his teaching diploma in Sciences (Math, Physics, and Computer Sciences) and his postgraduate diploma in Modeling and Stimulation at the Lebanese University, faculty of Sciences and Faculty of Engineers. Currently, he is preparing a PhD in Engineering Sciences at the Perpignan University Via Domitia.

Antonio Chahine received his Master degree in Energetic from the Lebanese University, Faculty of Sciences in 2017. He is working as a visiting student at the Laboratory of Applied Physics from 2016. His research interests include heat transfer, droplet evaporation and combustion.